Observational signatures of rotating black holes in the semiclassical gravity with trace anomaly

Zhenyu Zhang

School of Physics, Peking University

arXiv: 2305.14924

Collaborate with: Yehui Hou, Minyong Guo

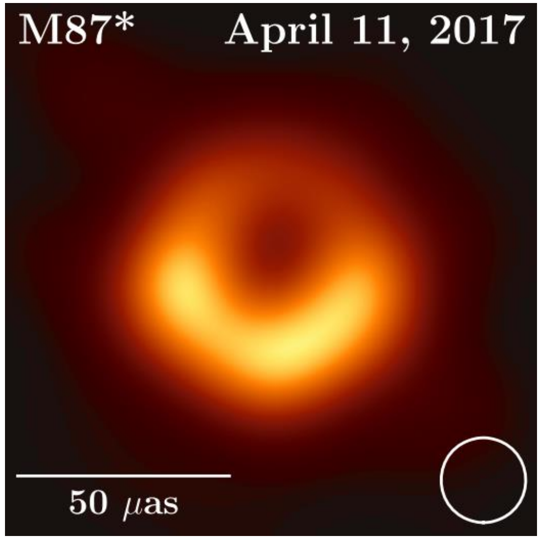

[1]

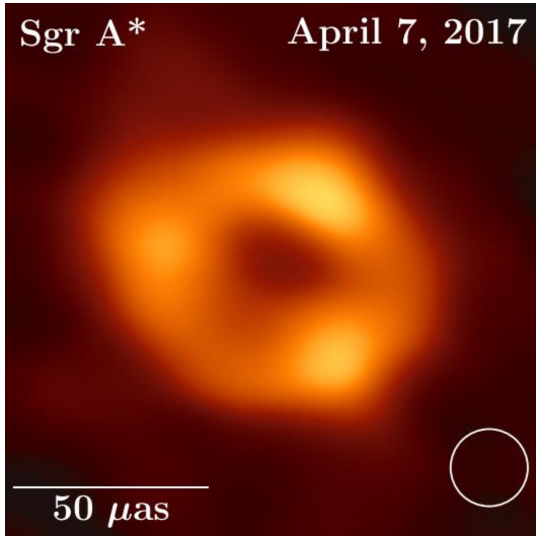

[2]

Spacetime information?

[1] The Event Horizon Telescope Collaboration et al. First M87 Event Horizon Telescope Results. Astrophys.J.Lett. 875 (2019).
[2] The Event Horizon Telescope Collaboration et al. First Sagittarius A* Event Horizon Telescope Results. Astrophys.J.Lett. 930 (2022).

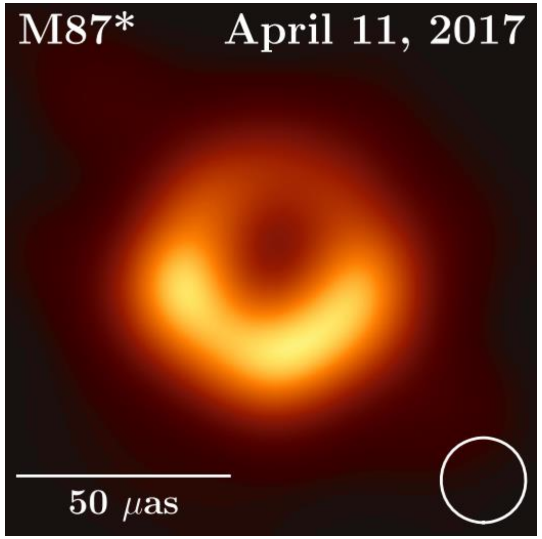

[1]

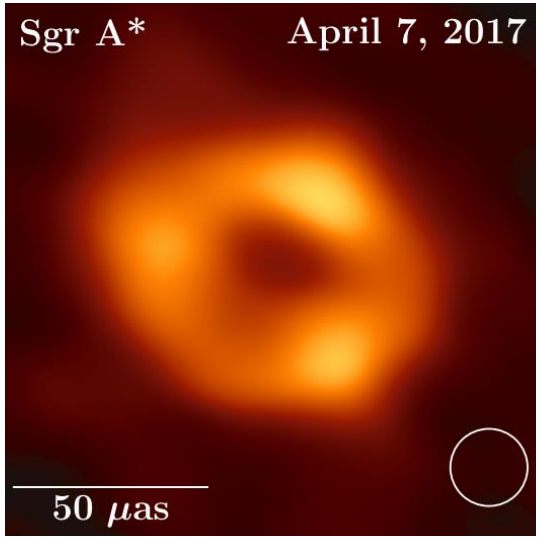

[2]

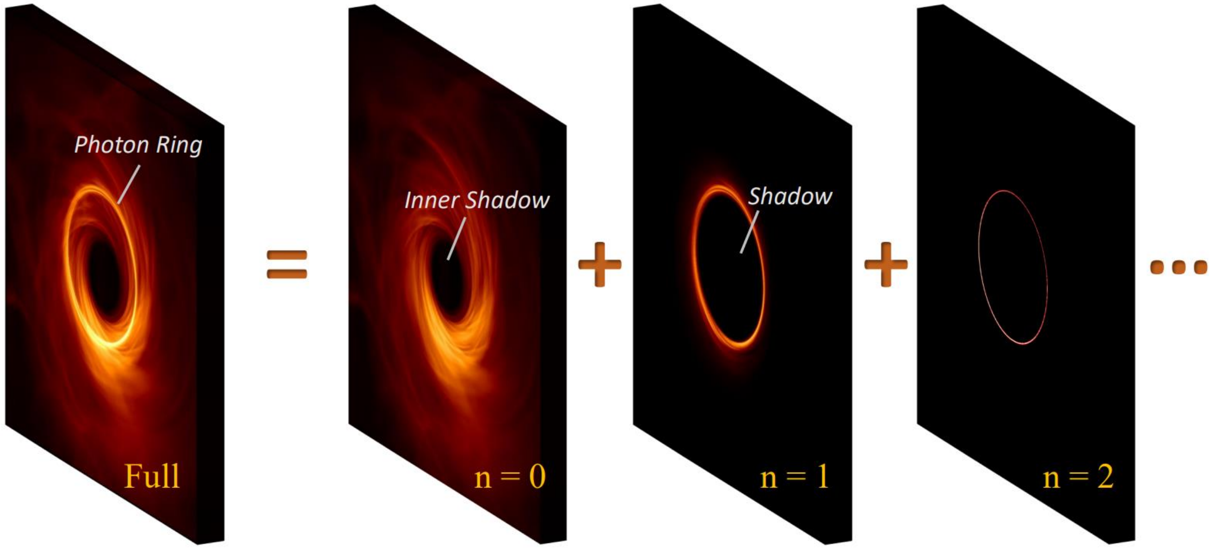

[3]

Photon ring (well-known) → High-order images

Spacetime information?

[1] The Event Horizon Telescope Collaboration et al. First M87 Event Horizon Telescope Results. Astrophys.J.Lett. 875 (2019).
[2] The Event Horizon Telescope Collaboration et al. First Sagittarius A* Event Horizon Telescope Results. Astrophys.J.Lett. 930 (2022).
[3] M. D. Johnson, K. Akiyama et al. Key Science Goals for the Next-Generation Event Horizon Telescope. Galaxies 11 (2023) 61.

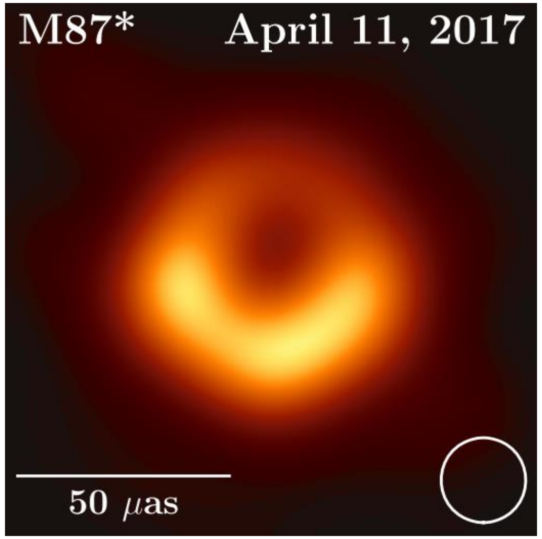

[1]

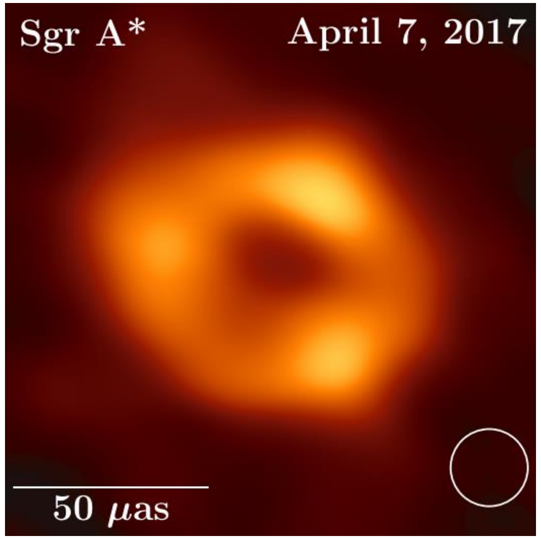

[2]

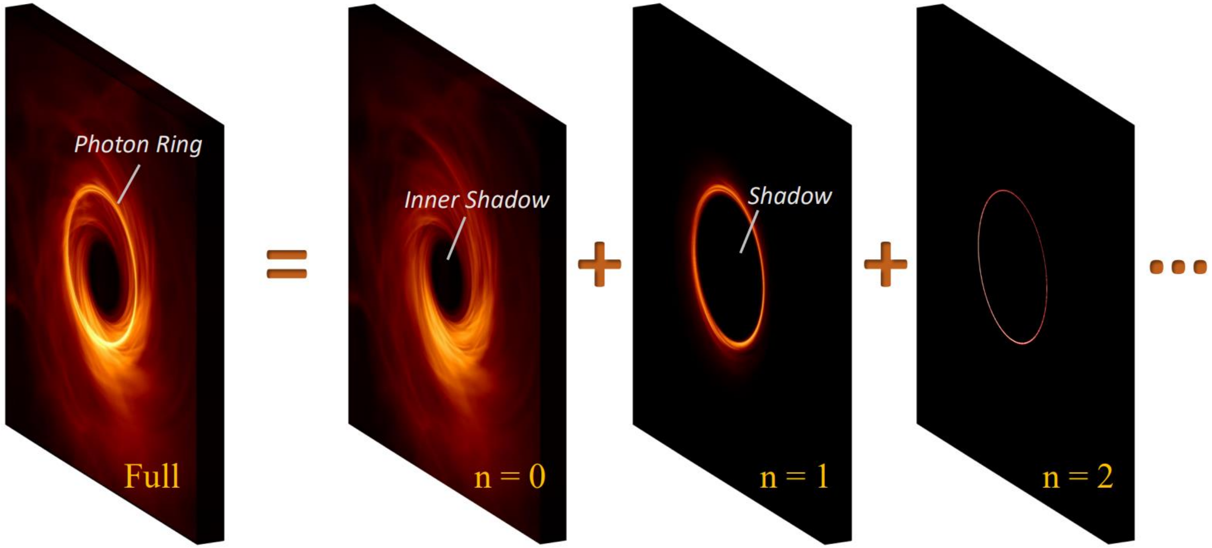

[3]

Photon ring (well-known) → High-order images

Spacetime information?

(in some cases)

Near-horizon source → Every-order images

[1] The Event Horizon Telescope Collaboration et al. First M87 Event Horizon Telescope Results. Astrophys.J.Lett. 875 (2019).
[2] The Event Horizon Telescope Collaboration et al. First Sagittarius A* Event Horizon Telescope Results. Astrophys.J.Lett. 930 (2022).
[3] M. D. Johnson, K. Akiyama et al. Key Science Goals for the Next-Generation Event Horizon Telescope. Galaxies 11 (2023) 61.

Contents

Background

- Type A trace anomaly [4, 5]

$$g^{\mu\nu} < T_{\mu\nu} > = \frac{\alpha}{2}(R^2 - 4R_{\mu\nu}R^{\mu\nu} + R_{\mu\nu\rho\sigma}R^{\mu\nu\rho\sigma})$$

- Semiclassical gravity

$$R^{\mu\nu} - \frac{1}{2}g^{\mu\nu}R = 8\pi G < T_{\mu\nu} >$$

- Black hole solution [6]

$$M = \frac{2m_0}{1 + \sqrt{1 - \frac{8\alpha r\xi m_0}{\Sigma^3}}}$$

$$\Sigma = r^2 + a^2\cos^2\theta$$
$$\xi = r^2 - 3a^2\cos^2\theta$$

[4] S. Deser and A. Schwimmer, Geometric classification of conformal anomalies in arbitrary dimensions, Phys. Lett. B 309 (1993) 279–284.
[5] D. M. Capper and M. J. Duff, Trace anomalies in dimensional regularization, Nuovo Cim. A 23 (1974) 173–183.
[6] P. G. S. Fernandes, Rotating black holes in semiclassical gravity, Phys. Rev. D 108 no. 6, (2023) L061502.

Light rings

- Effective potential

$$V_{eff}(r) \equiv \left(\frac{dr}{d\lambda}\right)^2 = E^2 - \mu^2 + \frac{2M\mu^2}{r} + \frac{a^2(E^2-\mu^2) - L^2}{r^2} + \frac{2M(L-aE)^2}{r^3}$$

- For photons

$$V_{eff}(r) = 1 + \frac{a^2 - l^2}{r^2} + \frac{2M(l-a)^2}{r^3}$$

- Light ring conditions

$$V_{eff} = 0, \qquad \partial_r V_{eff} = 0$$

- LRs are unstable

$$\partial_r^2 V_{eff} > 0$$

Light Rings

- Results

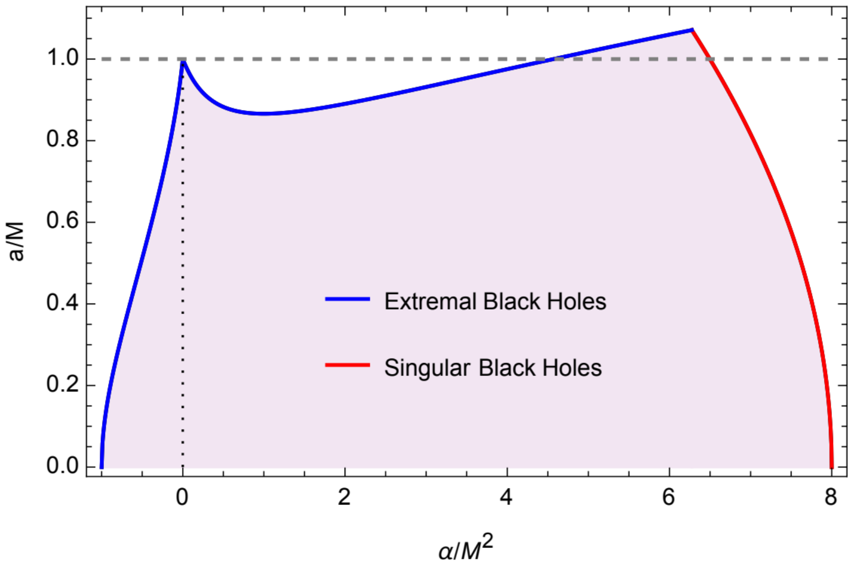

FIG. 2. Domain of existence for black hole solutions in the $(\alpha/M^2, a/M)$ plane. The shaded region represents the parameter space in which black hole solutions exist. The boundary of this region is formed by extremal (blue) and singular black holes (red).

[6]

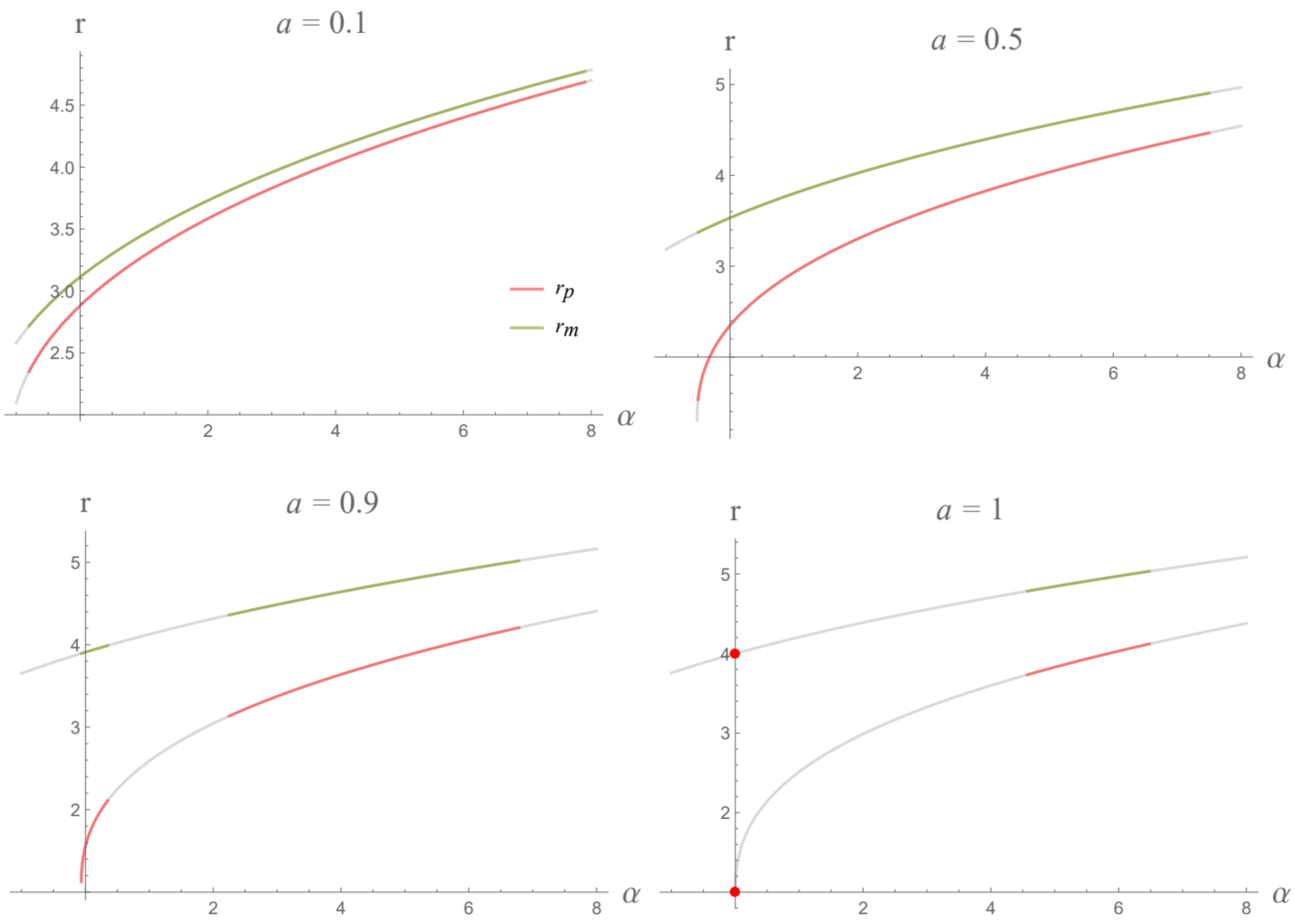

Figure 2: LRs as functions of α, under different spin parameters. The red and orange colors denote the prograde orbit and retrograde orbit, respectively.

[6] P. G. S. Fernandes, Rotating black holes in semiclassical gravity, Phys. Rev. D 108 no. 6, (2023) L061502.

Black hole shadows

- Celestial light source & ray tracing

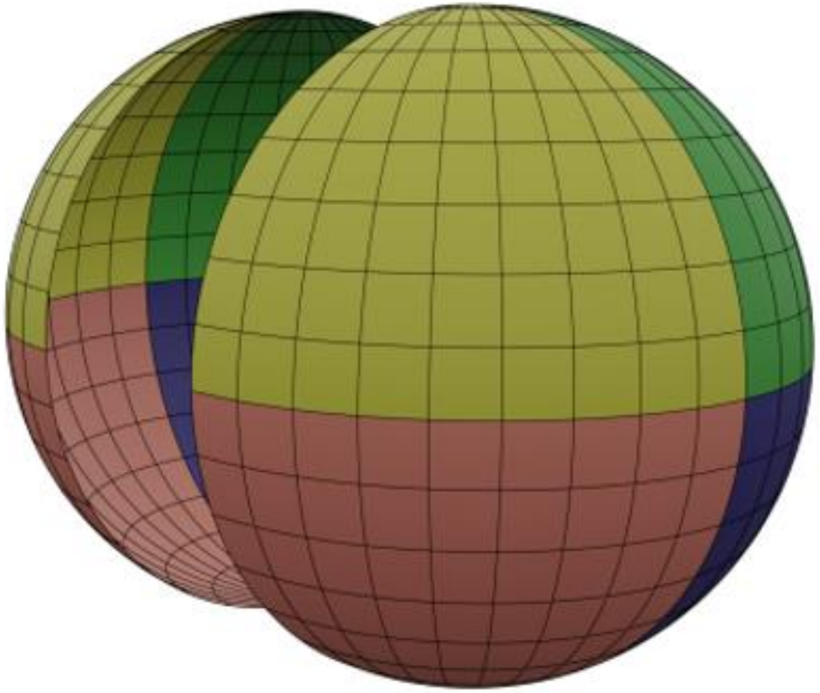

[7]

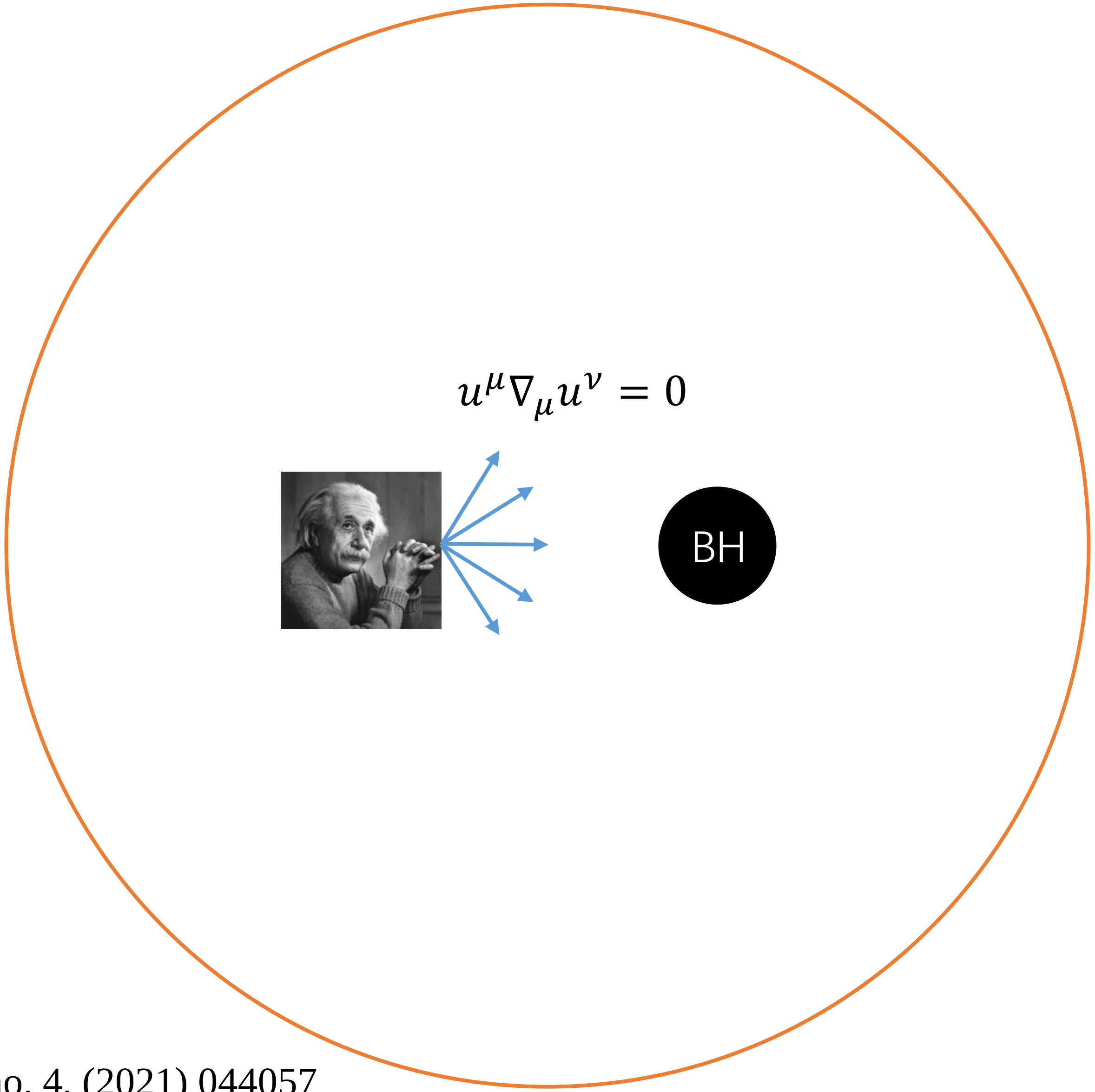

[7] Z. Hu et al. QED effect on a black hole shadow, Phys. Rev. D 103 no. 4, (2021) 044057

Black hole shadows

- Celestial light source & ray tracing

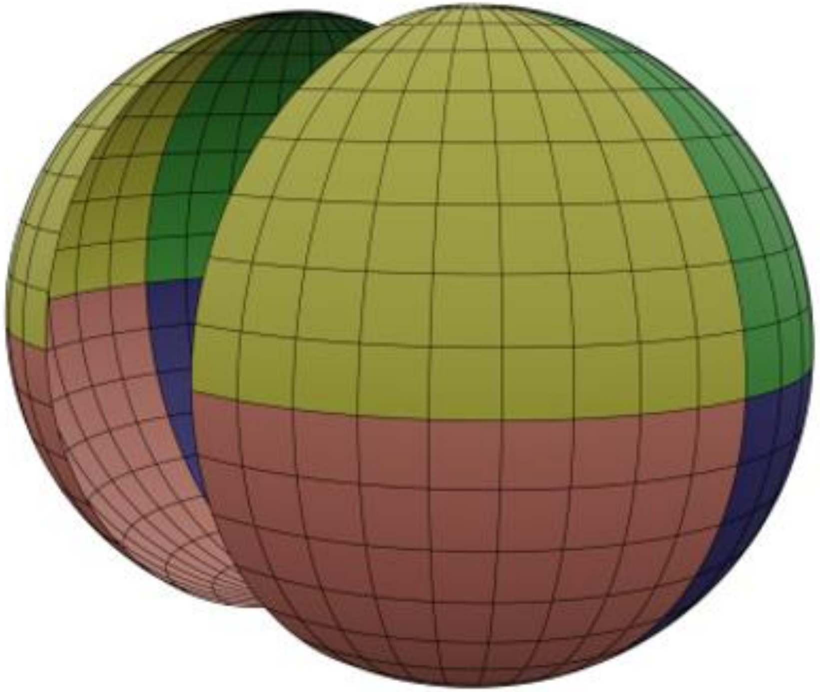

[7]

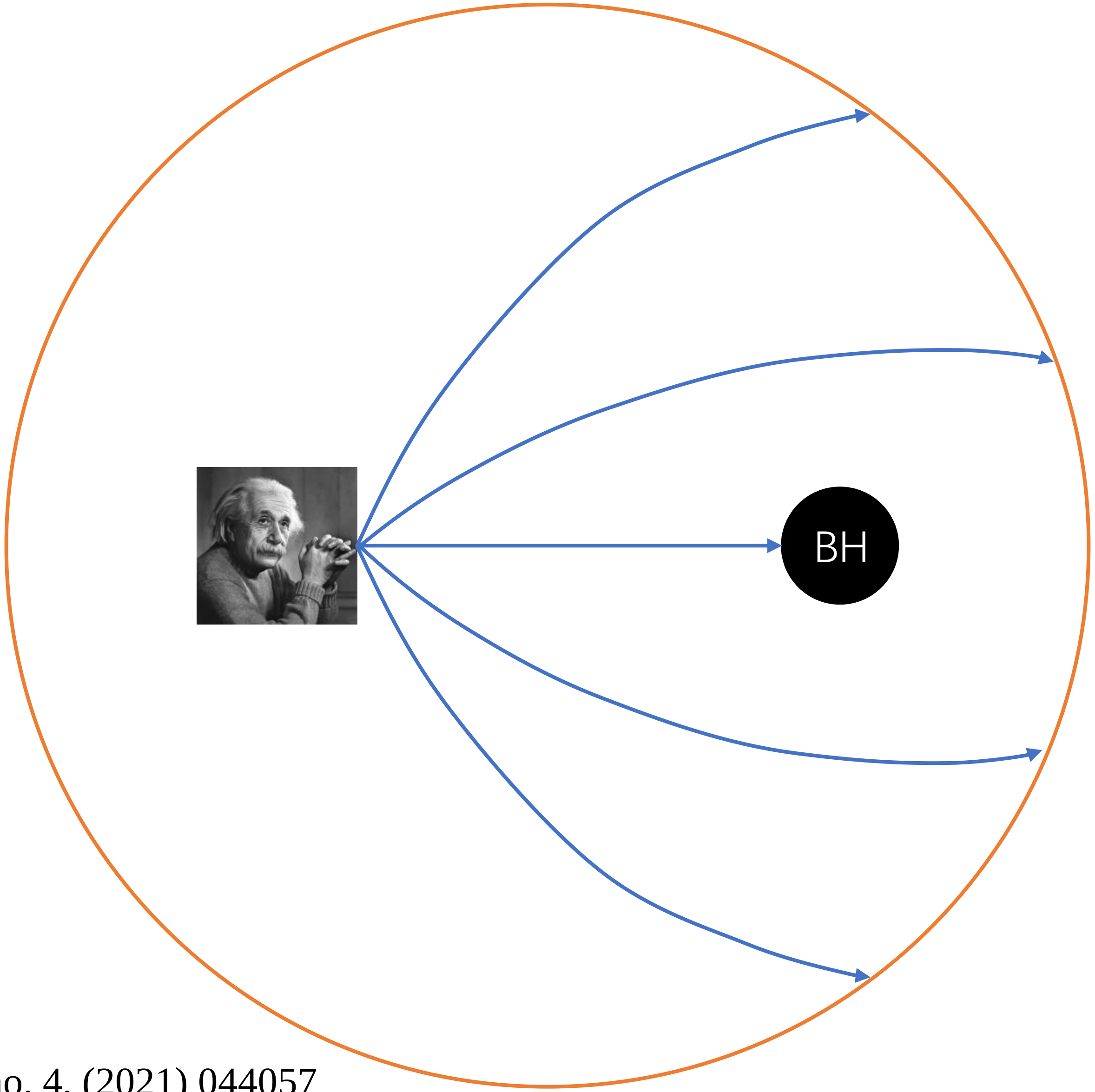

[7] Z. Hu et al. QED effect on a black hole shadow, Phys. Rev. D 103 no. 4, (2021) 044057

Black hole shadows

- Celestial light source & ray tracing

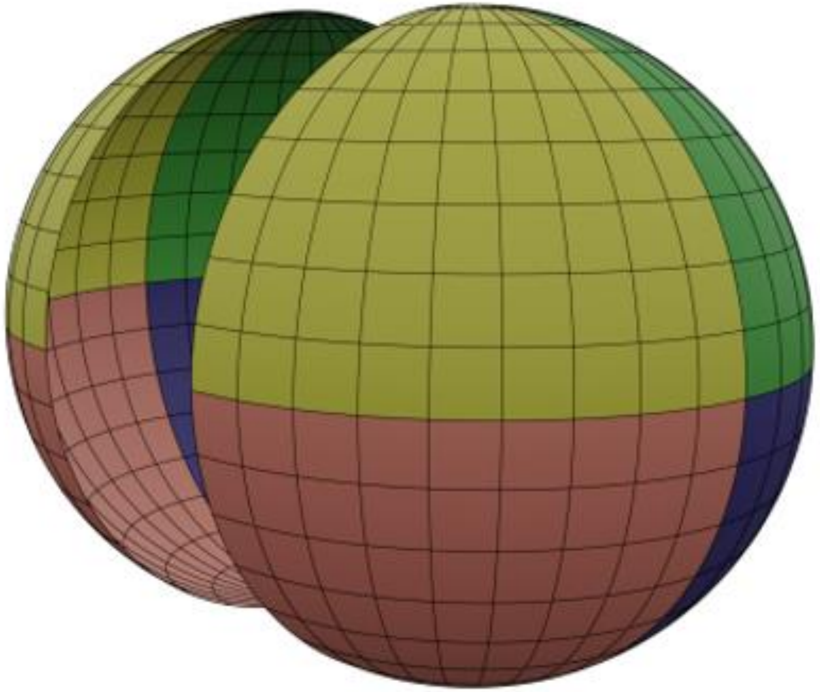

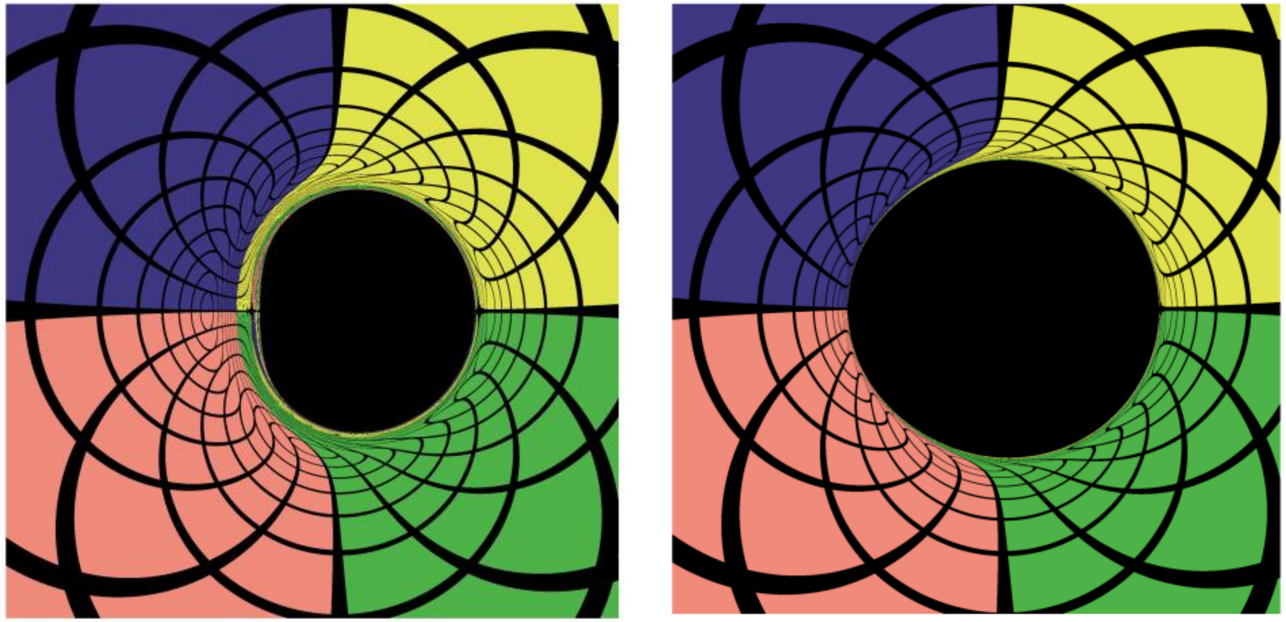

[7]

[7] Z. Hu et al. QED effect on a black hole shadow, Phys. Rev. D 103 no. 4, (2021) 044057

Black hole shadows

- Main results
  - For high-spin case, NHEK line [8] disappear

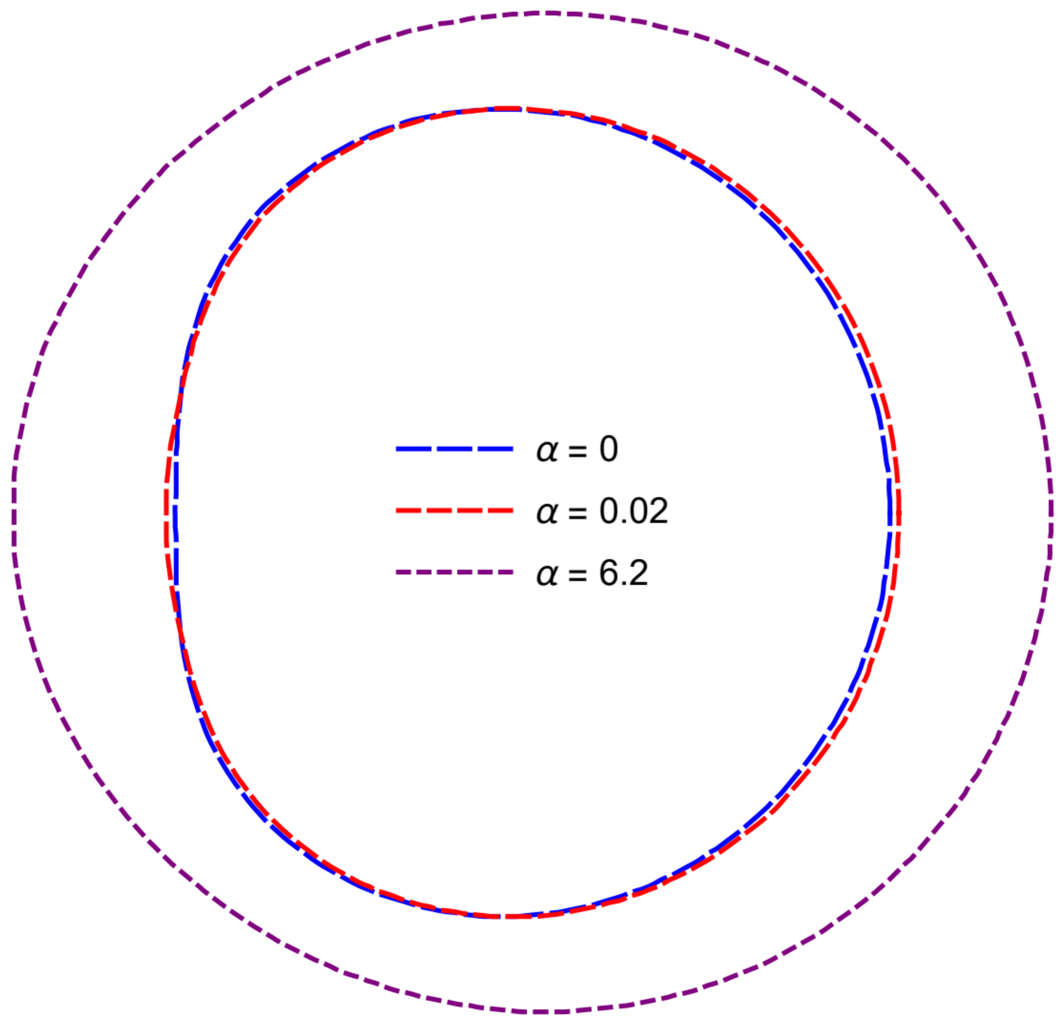

$a = 0.99, \theta_o = 90°$

[8] S. E. Gralla, A. Lupsasca, and A. Strominger, Observational Signature of High Spin at the Event Horizon Telescope, Mon. Not. Roy. Astron. Soc. 475 no. 3, (2018) 3829–3853.

Black hole shadows

- Main results
  - For high-spin case, NHEK line disappear

NHEK line [8] :

An edge-on observer can observe a vertical line segment within the left contour of the shadow.

↑

Near-Horizon-Extreme-Kerr geometry

↑

Global degeneracy of the horizons ($r_+ = r_-$) [9]

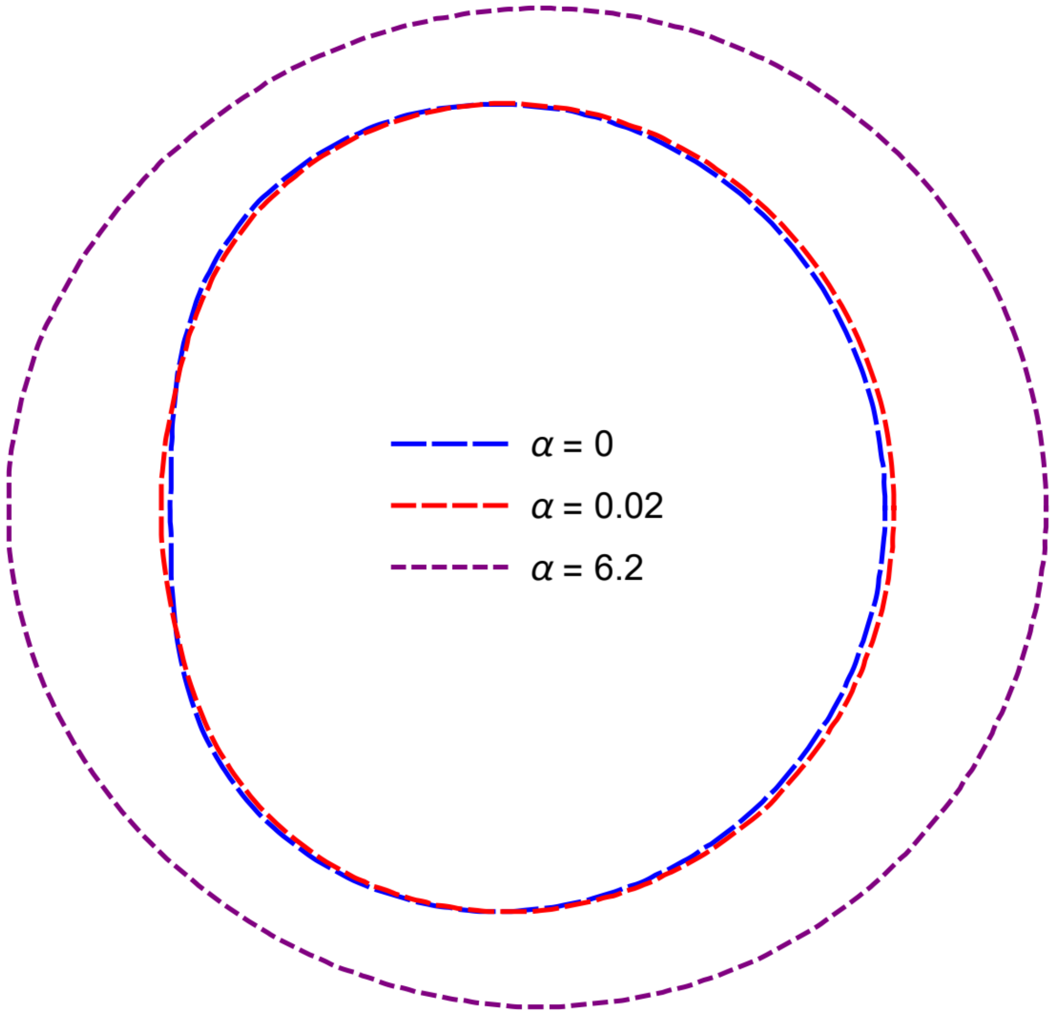

$a = 0.99, \theta_o = 90°$

[8] S. E. Gralla, A. Lupsasca, and A. Strominger, Observational Signature of High Spin at the Event Horizon Telescope, Mon. Not. Roy. Astron. Soc. 475 no. 3, (2018) 3829–3853.

[9] J. M. Bardeen and G. T. Horowitz, The Extreme Kerr throat geometry: A Vacuum analog of AdS(2) x S**2, Phys. Rev. D 60 (1999) 104030.

Black hole shadows

- Main results
  - For high-spin case, NHEK line disappear

NHEK line [8] :

An edge-on observer can observe a vertical line segment within the left contour of the shadow.

Near-Horizon-Extreme-Kerr geometry

Global degeneracy of the horizons $(r_+ = r_-)$ [9]

Quantum correction (parameter α)

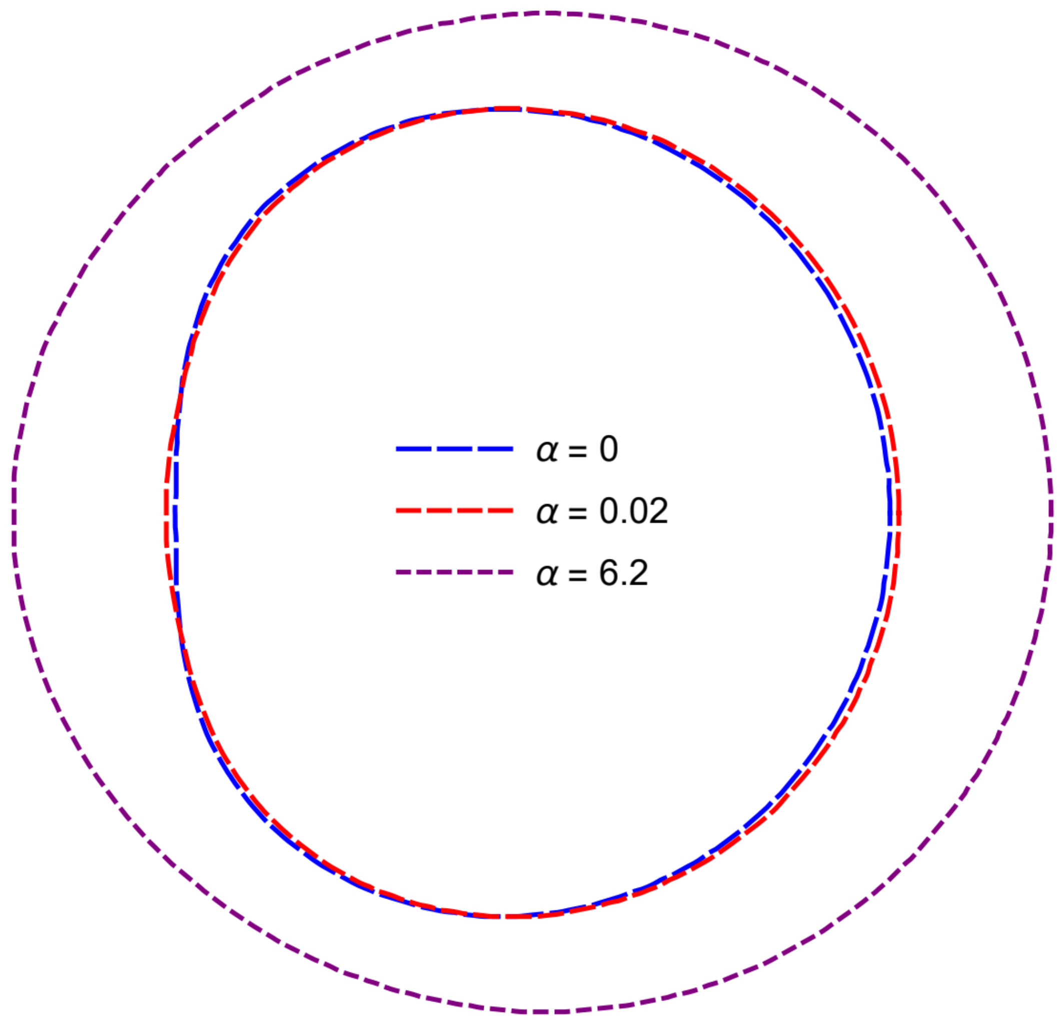

$a = 0.99, \theta_o = 90°$

[8] S. E. Gralla, A. Lupsasca, and A. Strominger, Observational Signature of High Spin at the Event Horizon Telescope, Mon. Not. Roy. Astron. Soc. 475 no. 3, (2018) 3829–3853.

[9] J. M. Bardeen and G. T. Horowitz, The Extreme Kerr throat geometry: A Vacuum analog of AdS(2) x S**2, Phys. Rev. D 60 (1999) 104030.

Black hole shadows

- Main results
  - For high-spin case, NHEK line disappear

NHEK line [8] :

An edge-on observer can observe a vertical line segment within the left contour of the shadow.

↑

Near-Horizon-Extreme-Kerr geometry

↑

Global degeneracy of the horizons ($r_+ = r_-$) [9]

↑

Quantum correction (parameter α)

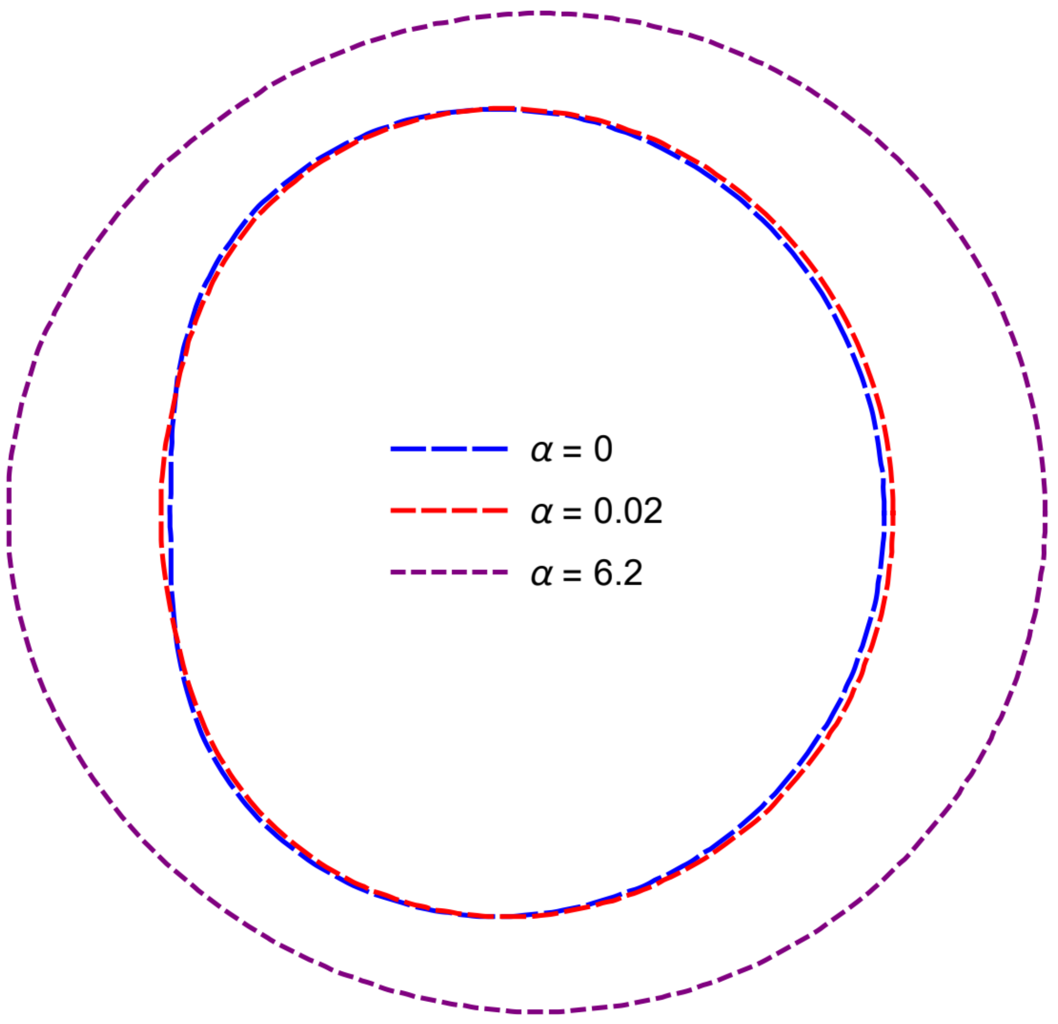

$a = 0.99, \theta_o = 90°$

[8] S. E. Gralla, A. Lupsasca, and A. Strominger, Observational Signature of High Spin at the Event Horizon Telescope, Mon. Not. Roy. Astron. Soc. 475 no. 3, (2018) 3829–3853.

[9] J. M. Bardeen and G. T. Horowitz, The Extreme Kerr throat geometry: A Vacuum analog of AdS(2) x S**2, Phys. Rev. D 60 (1999) 104030.

Black hole shadows

- Main results
  - For high-spin case, NHEK line disappear
  - Area ratio $\eta \equiv S_{BH}/S_{Kerr}$
    - Monotonically increasing function of quantum-corrected parameter α

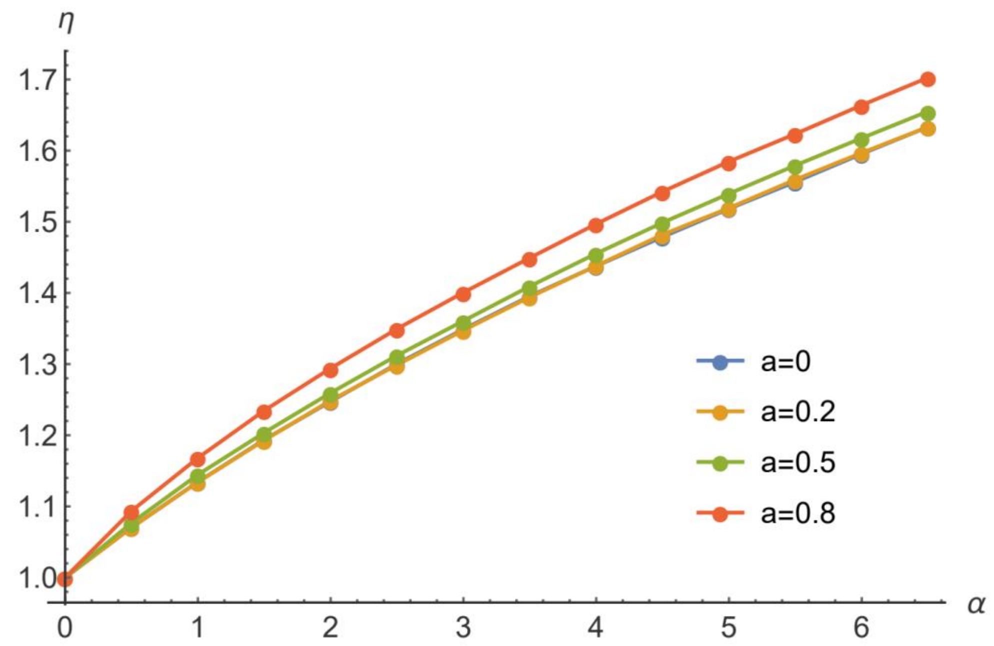

$\alpha \geq 0, \theta_o = 90°$

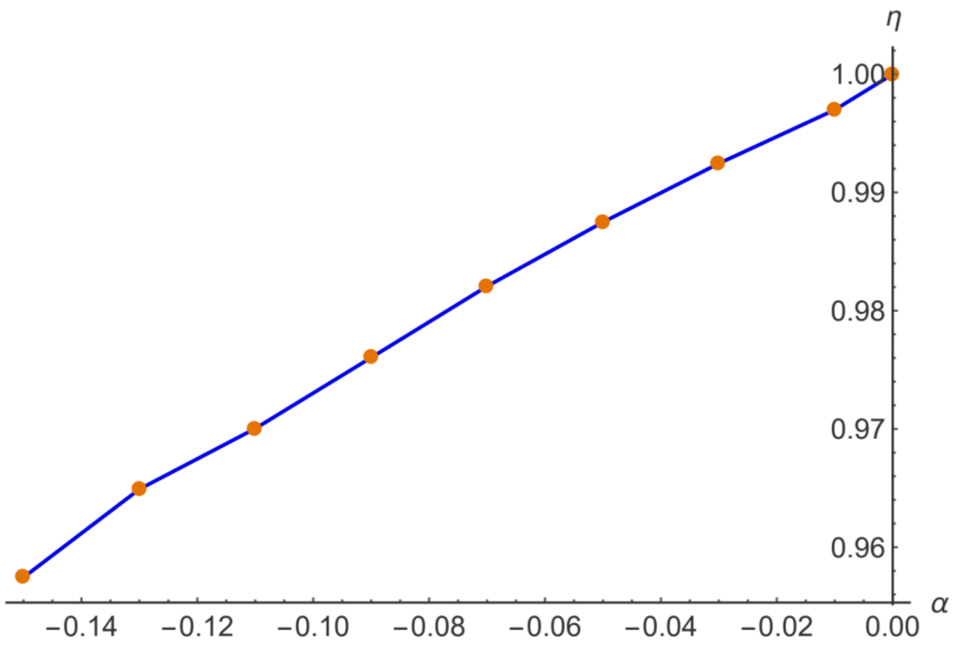

$\alpha \leq \ 0, a = 0.8, \theta_o = 90°$

Images with a thin disk

- Disk model (geometrically and optically thin)
  - placed on the equatorial plane
  - Outside the ISCO: circular orbits
  - Inside the ISCO: falls from the ISCO to the horizon

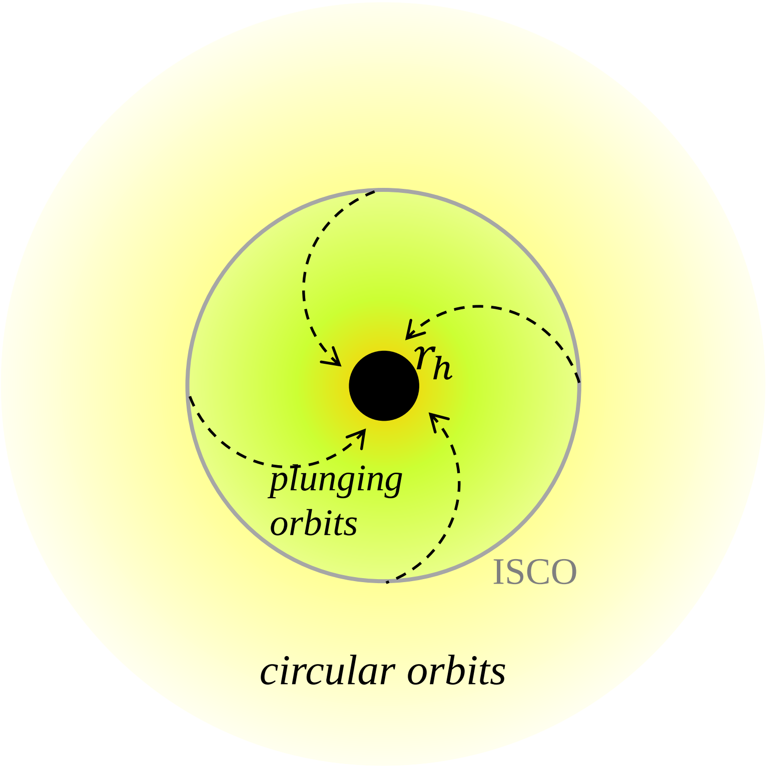

Images with a thin disk

- Disk model (geometrically and optically thin)
  - placed on the equatorial plane
  - Outside the ISCO: circular orbits
  - Inside the ISCO: falls from the ISCO to the horizon

  - Emissivity [10] $$J = \exp\left(-\frac{1}{2}z^2 - 2z\right)$$
$$z = \ln\left(\frac{r}{r_H}\right)$$

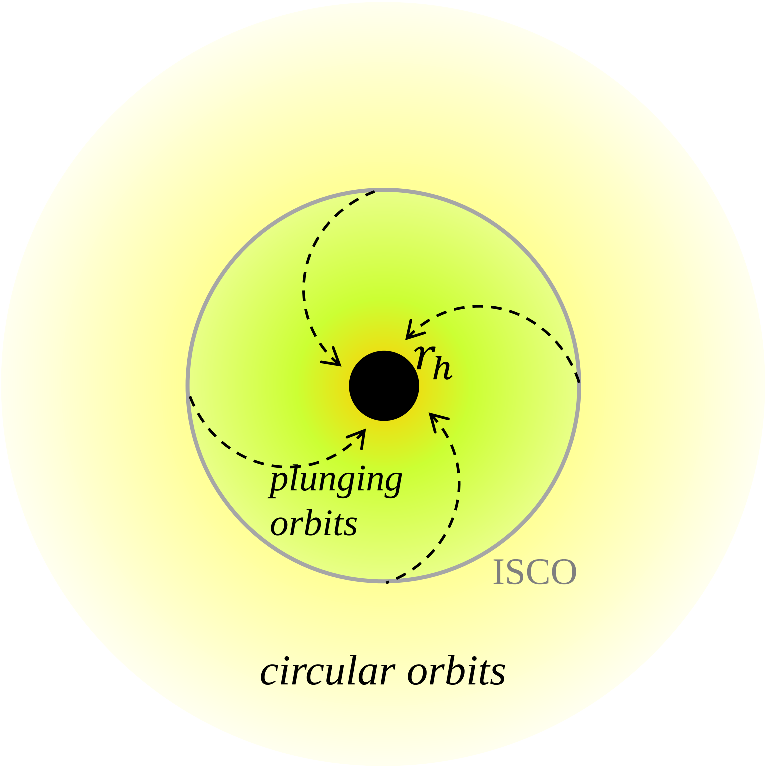

[10] A. Chael et al. Observing the Inner Shadow of a Black Hole: A Direct View of the Event Horizon, Astrophys. J. 918 no. 1, (2021) 6.

Images with a thin disk

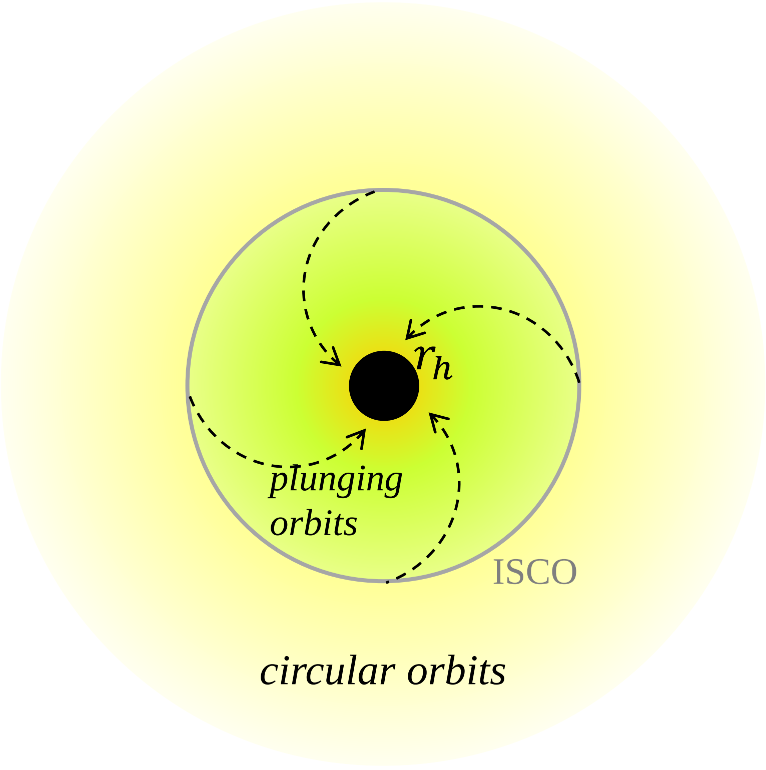

- Disk model (geometrically and optically thin)
  - placed on the equatorial plane
  - Outside the ISCO: circular orbits
  - Inside the ISCO: falls from the ISCO to the horizon

- Emissivity [10]

$$J = \exp\left(-\frac{1}{2}z^2 - 2z\right)$$

$$z = \ln\left(\frac{r}{r_H}\right)$$

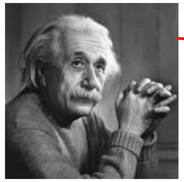

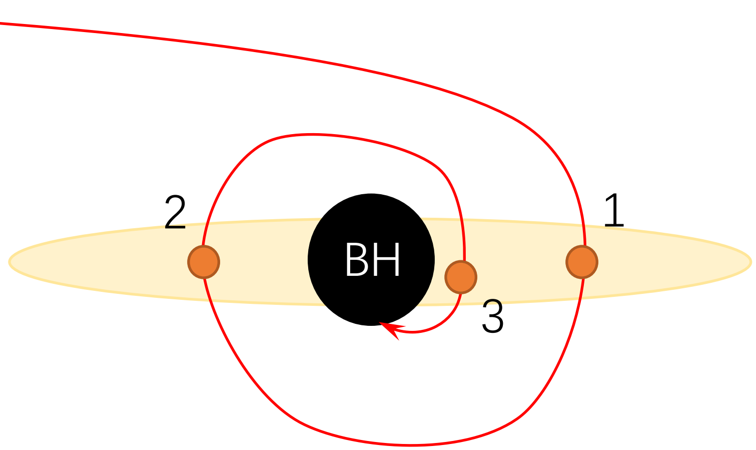

- Intensity

$$I_{\nu_o} = \sum_{n=1}^{N} g_n^3 J_n$$

[10] A. Chael et al. Observing the Inner Shadow of a Black Hole: A Direct View of the Event Horizon, Astrophys. J. 918 no. 1, (2021) 6.

Images with a thin disk

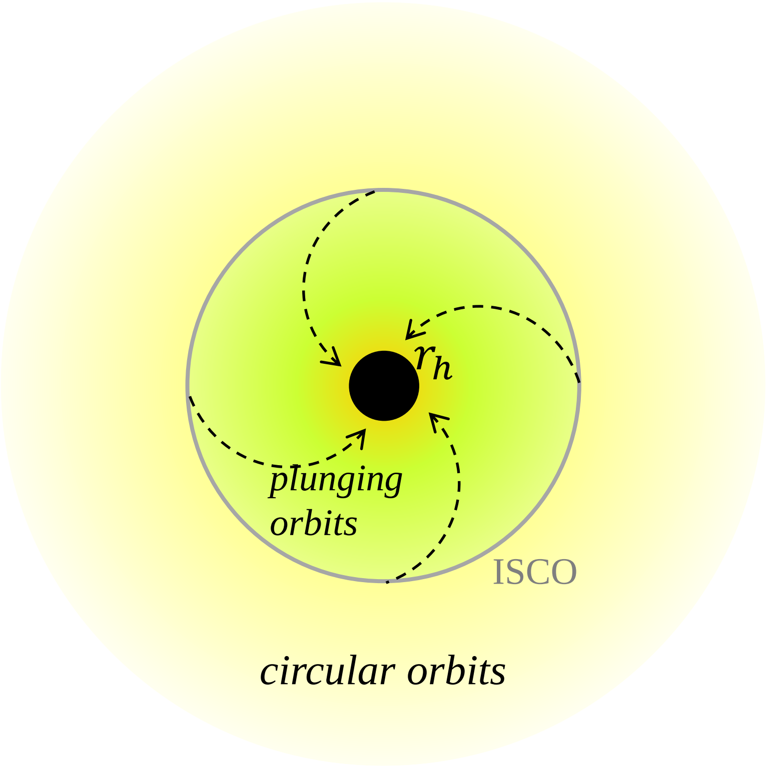

- Disk model (geometrically and optically thin)
  - placed on the equatorial plane
  - Outside the ISCO: circular orbits
  - Inside the ISCO: falls from the ISCO to the horizon

- Emissivity [10] $$J = \exp\left(-\frac{1}{2}z^2 - 2z\right)$$ $$z = \ln\left(\frac{r}{r_H}\right)$$

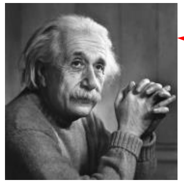

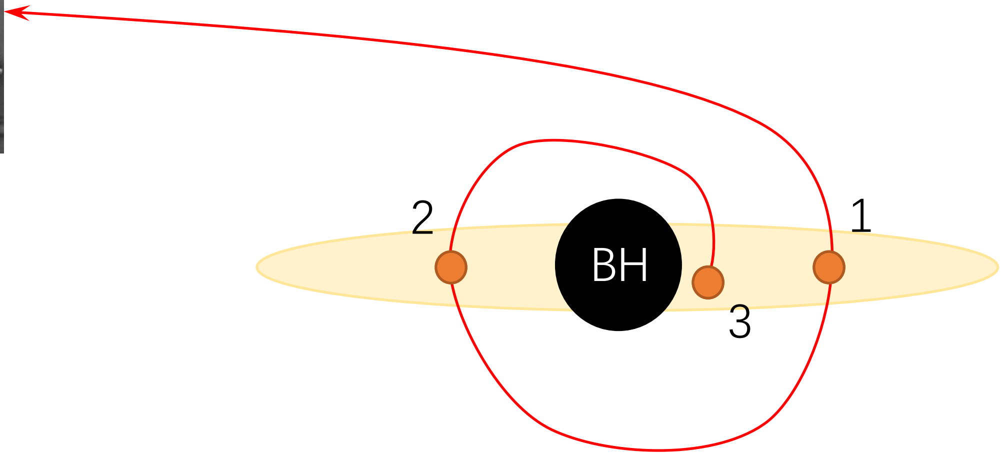

- Intensity $$I_{\nu_o} = \sum_{n=1}^{N} g_n^3 J_n$$

[10] A. Chael et al. Observing the Inner Shadow of a Black Hole: A Direct View of the Event Horizon, Astrophys. J. 918 no. 1, (2021) 6.

Images with a thin disk

- Results
  - Intensity : a smaller *inner shadow* [10]

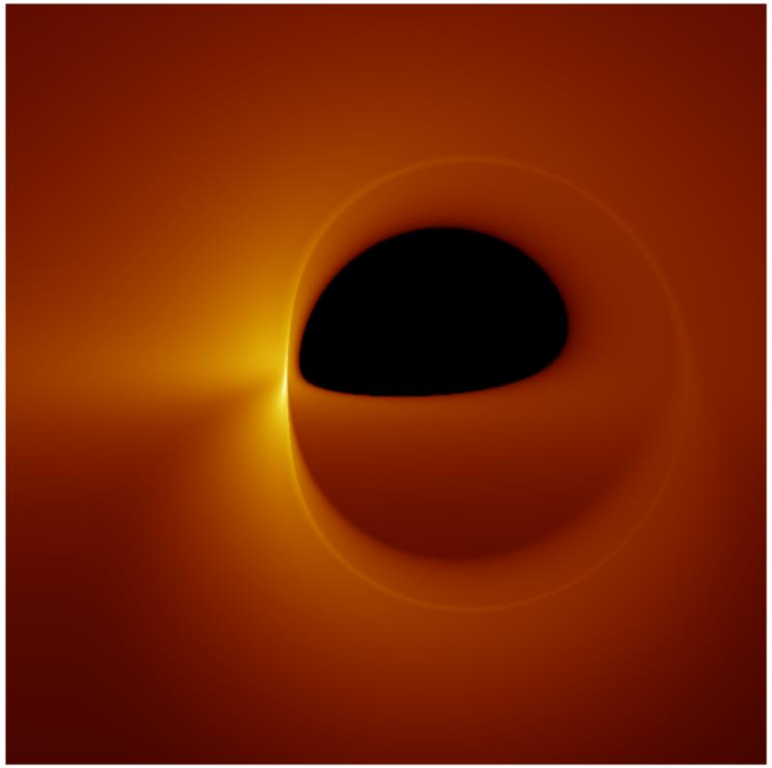

$a = 0.99, \alpha = 0, \theta_o = 80°$

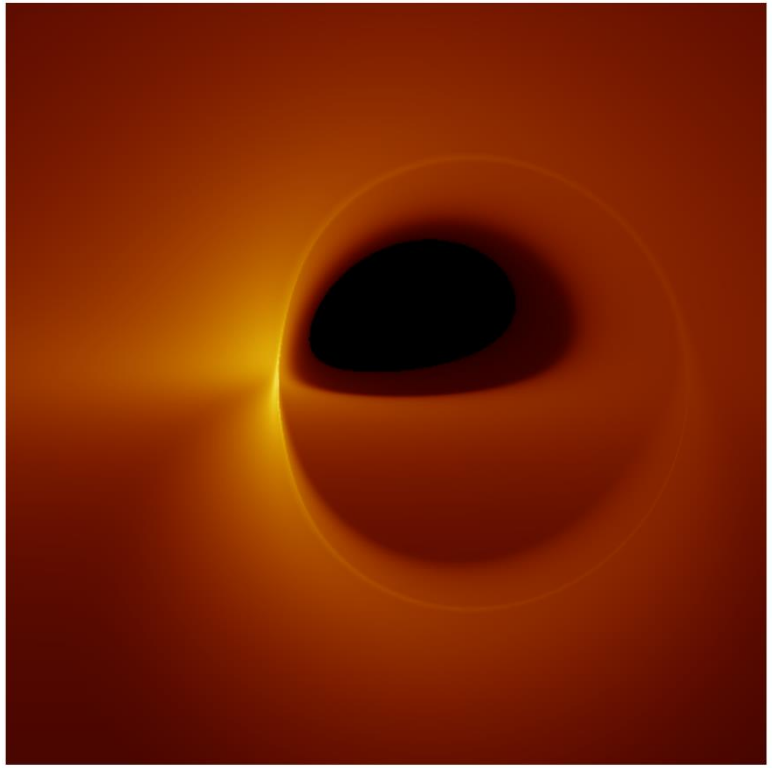

$a = 0.99, \alpha = 0.02, \theta_o = 80°$

[10] A. Chael et al. Observing the Inner Shadow of a Black Hole: A Direct View of the Event Horizon, Astrophys. J. 918 no. 1, (2021) 6.

Images with a thin disk

- Results
  - Number of times the light rays intersect the disk

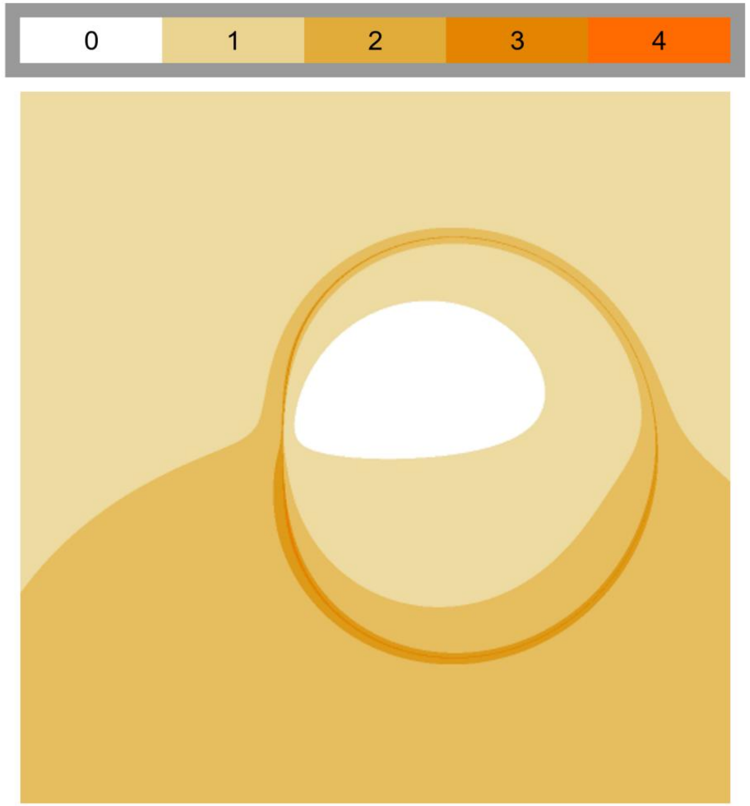

$a = 0.99, \alpha = 0, \theta_o = 80°$

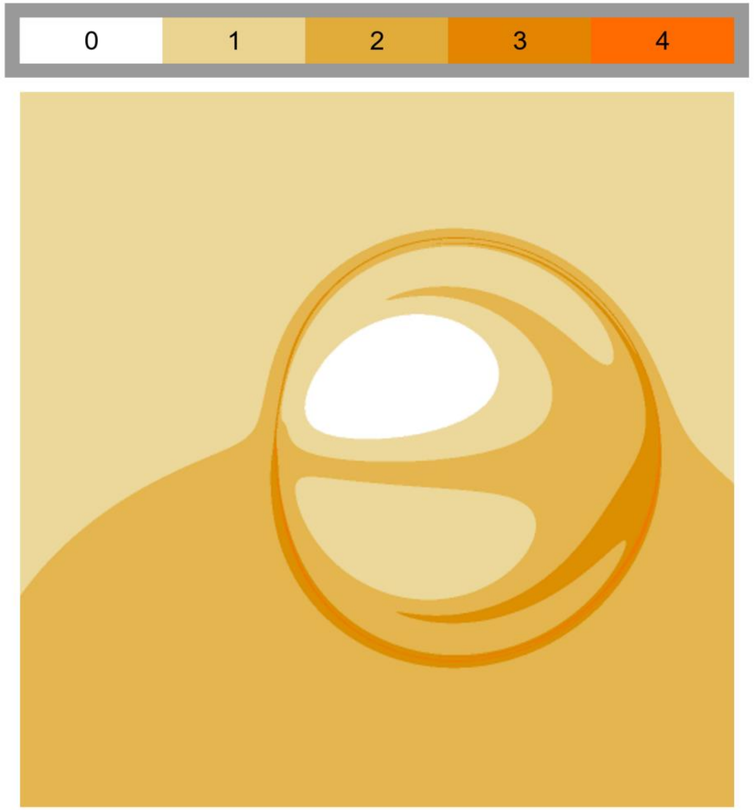

$a = 0.99, \alpha = 0.02, \theta_o = 80°$

Images with a thin disk

- Results
  - Only inner-ISCO region

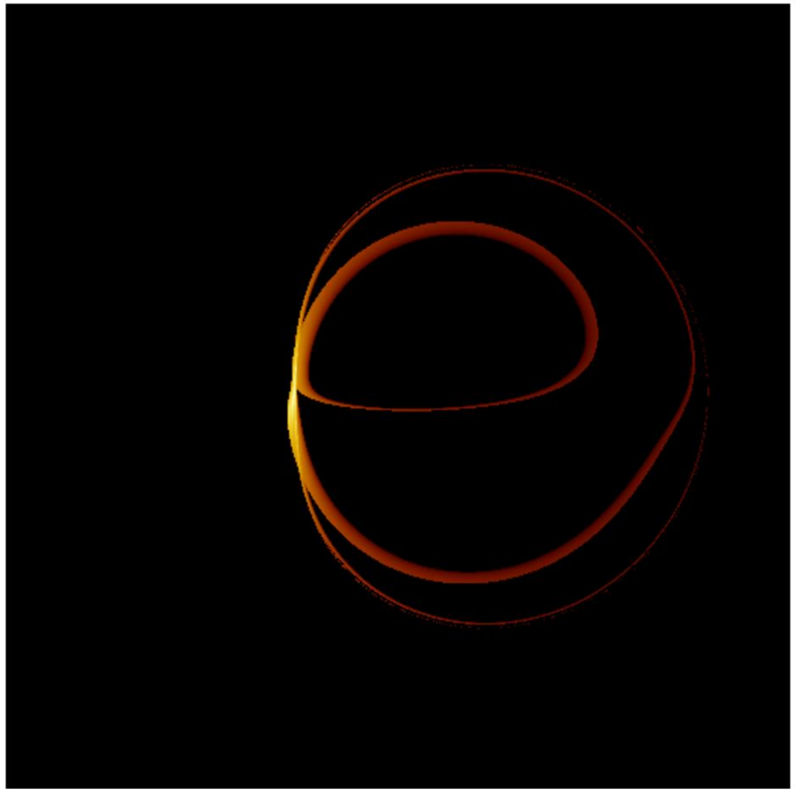

$a = 0.99, \alpha = 0, \theta_o = 80°$

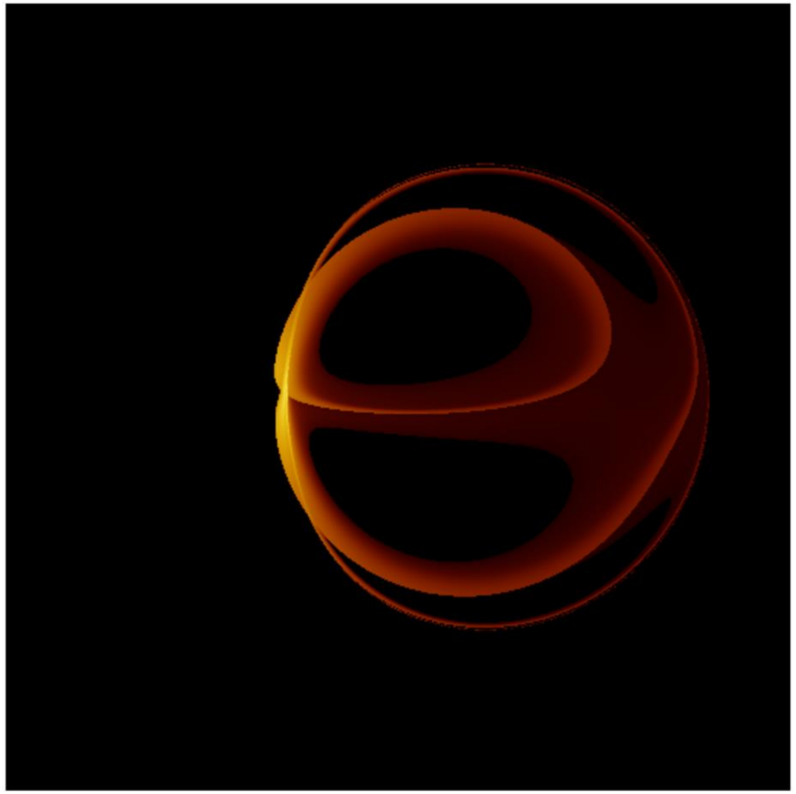

$a = 0.99, \alpha = 0.02, \theta_o = 80°$

Summary

- We explore the observational signature of a rotating black holes in the semiclassical gravity with trace anomaly.
- For high-spin black holes, the NHEK line was highly susceptible to disruption by the quantum correction effect.
- Our study highlights the importance of near-horizon emission sources in detecting the effects of quantum corrections by black hole images.

See our paper
(arXiv:2305.14924)
for more details

Thanks for listening!

Appendix

$$u^\mu = u^t_{\rm out}(1\,,0\,,0\,,\Omega_s)\,,$$

where

$$u^t_{\rm out} = \sqrt{-\frac{1}{g_{\phi\phi}\Omega_s^2 + 2g_{t\phi}\Omega_s + g_{tt}}}\,\Bigg|_{\theta=\pi/2}\,, \quad \Omega_s = \frac{-\partial_r g_{t\phi} + \sqrt{(\partial_r g_{t\phi})^2 - \partial_r g_{\phi\phi}\partial_r g_{tt}}}{\partial_r g_{\phi\phi}}\,\Bigg|_{\theta=\pi/2}\,.$$

$$u^t_{\rm in} = (-g^{tt}E_{\rm ISCO} + g^{t\phi}L_{\rm ISCO})\,\big|_{\theta=\pi/2}\,, \quad u^\phi_{\rm in} = (-g^{t\phi}E_{\rm ISCO} + g^{\phi\phi}L_{\rm ISCO})\,\big|_{\theta=\pi/2}\,,$$

$$u^r_{\rm in} = -\sqrt{-\frac{g_{tt}u^t_{\rm in}u^t_{\rm in} + 2g_{t\phi}u^t_{\rm in}u^\phi_{\rm in} + g_{\phi\phi}u^\phi_{\rm in}u^\phi_{\rm in} + 1}{g_{rr}}}\,\Bigg|_{\theta=\pi/2}\,, \quad u^\theta_{\rm in} = 0\,,$$

where $E_{\rm ISCO}$ and $L_{\rm ISCO}$ is the conserved energy and angular momentum at the ISCO.

See our paper
(arXiv:2305.14924)
for more details

Thanks for listening!

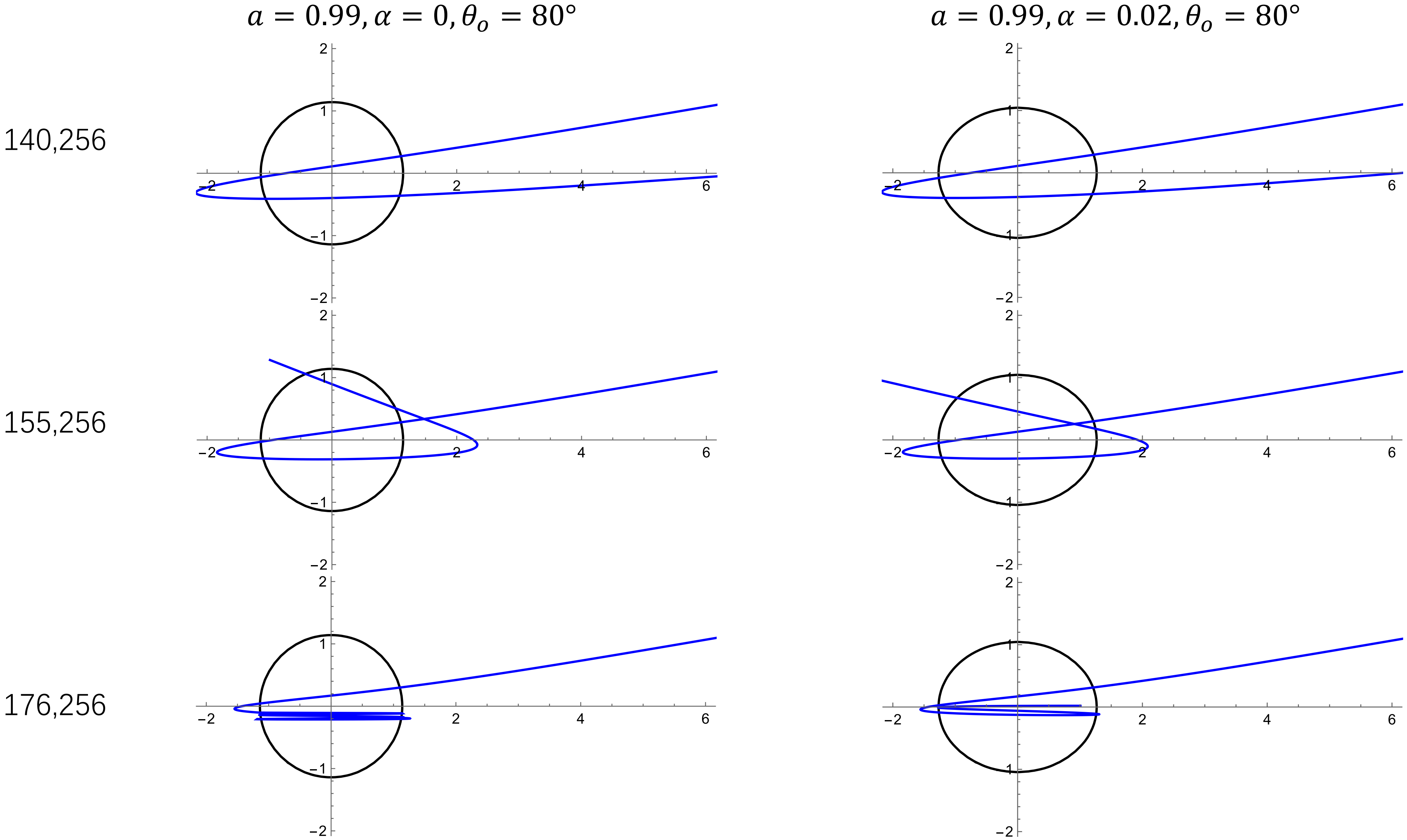

$a = 0.99, \alpha = 0, \theta_o = 80°$
$a = 0.99, \alpha = 0.02, \theta_o = 80°$
140,256
155,256
176,256

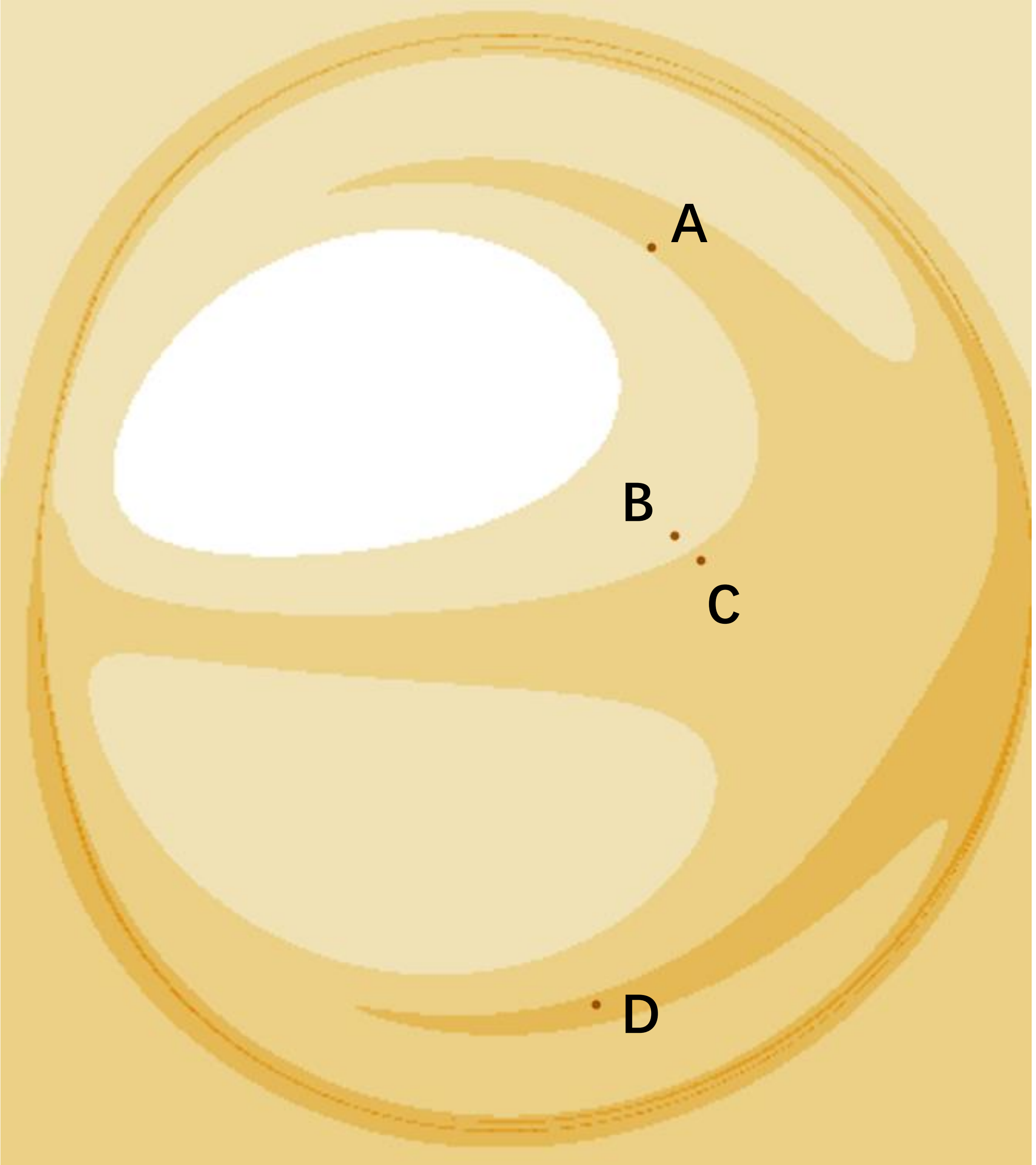
A
B
C
D

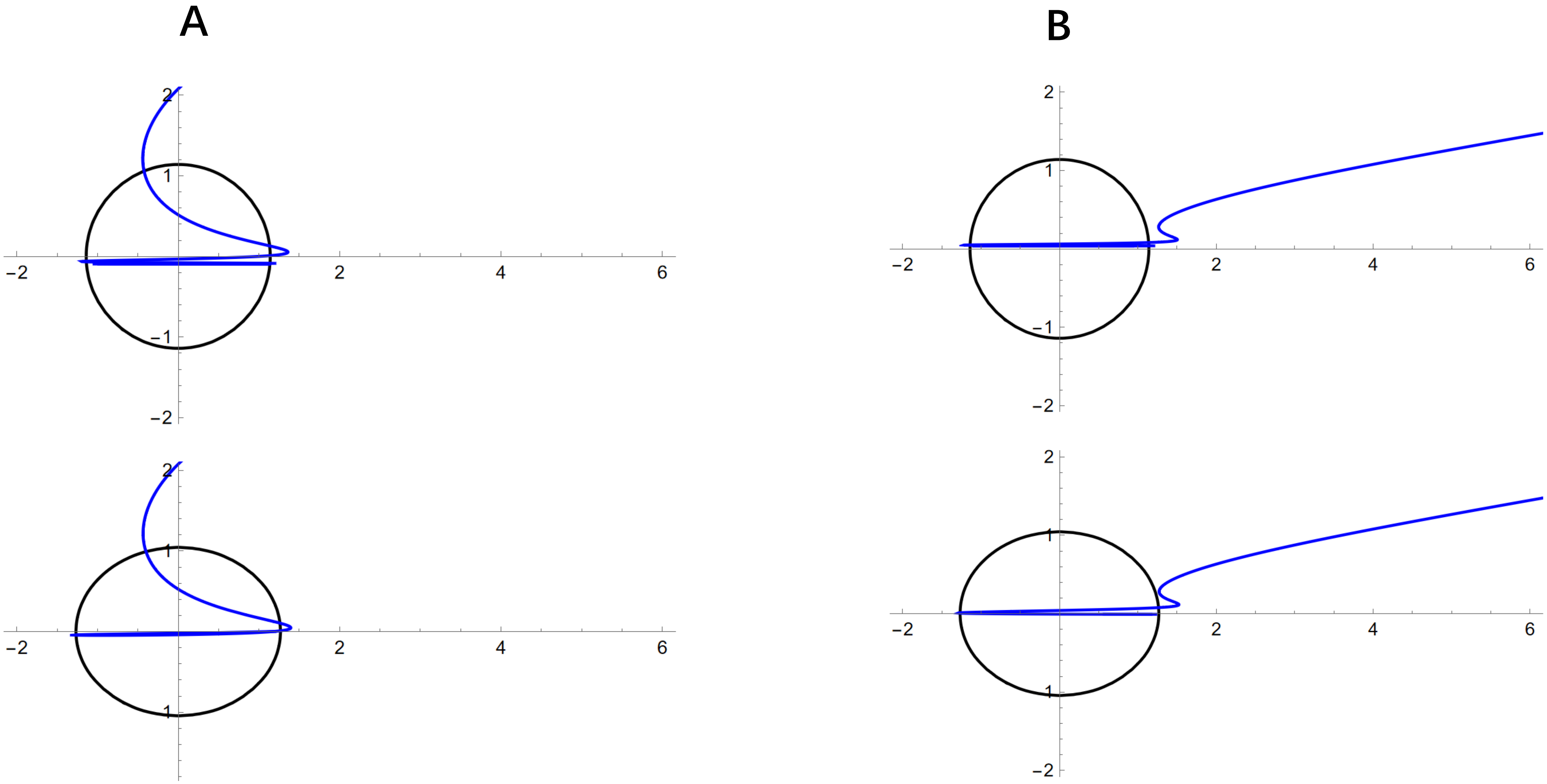

A
B
−2
2
4
6
2
1
−1
−2

C

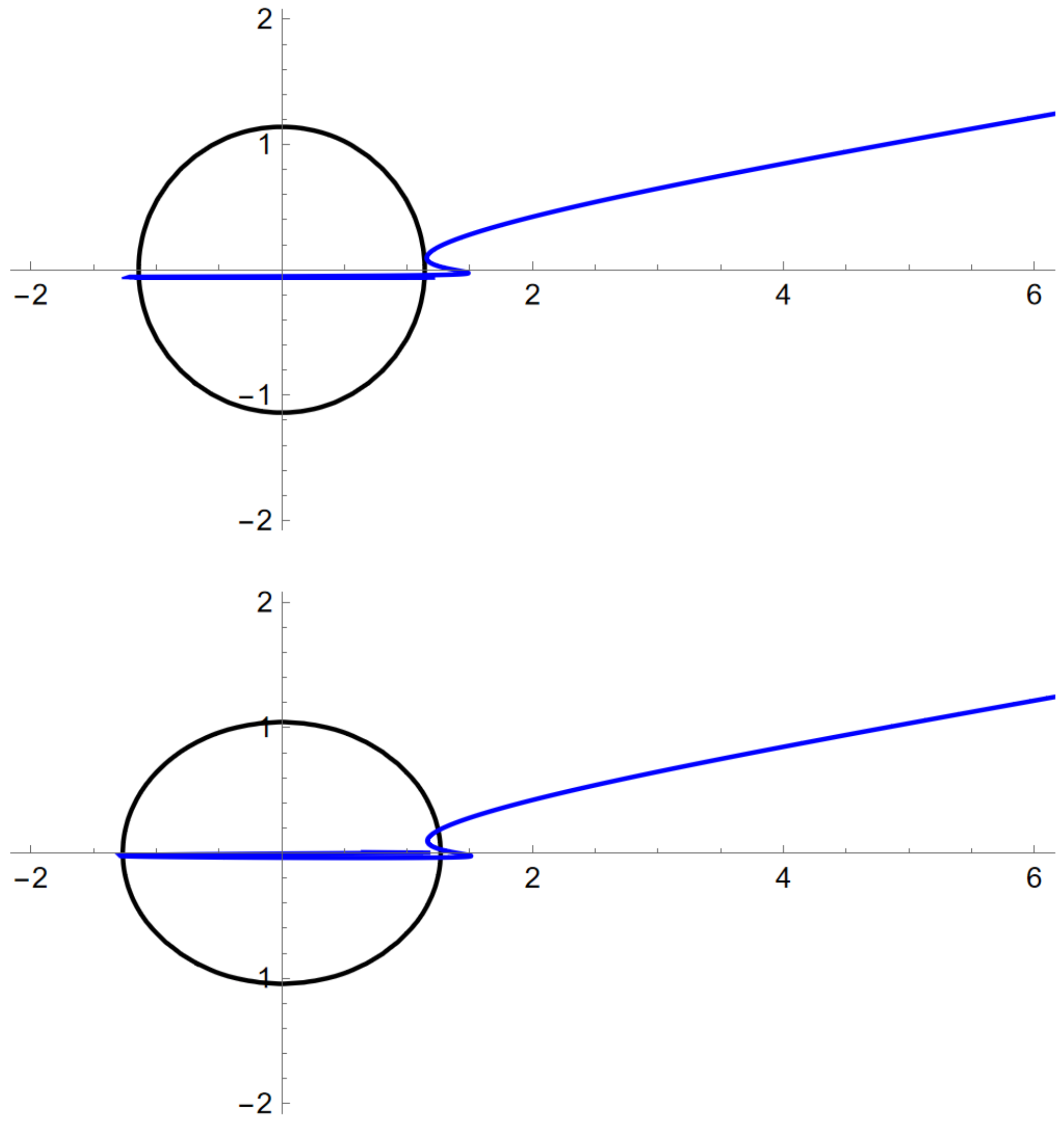

D